

Spontaneous synchronization of metronomes on a freely rotating platform

Sz. Boda, Z. Néda, B. Tyukodi and A. Tunyagi

*Babes-Bolyai University, Department of Physics,
str. Kogălniceanu 1 nr. 1, 400084, Cluj-Napoca, Romania*

(Dated: October 12, 2012)

Spontaneous synchronization of an ensemble of metronomes placed on a freely rotating platform is studied experimentally and by computer simulations. The experiments revealed that independently of the initial conditions and metronome numbers on the platform, only in-phase synchronization is observable. The conditions favoring the emergence of this collective behavior is investigated. It is found that there is a limiting natural frequency of the metronomes below which spontaneous synchronization is not observable. Increasing the number of metronomes on the platform leads to a decreasing trend in the synchronization level and a longer time to achieve this.

I. INTRODUCTION

Spontaneous synchronization of coupled non-identical oscillators is a well-known form of collective behavior [1–6]. The problem has been intensively studied since Huygens, and if the legend is true he was the first one who noticed and reported the synchronized swinging of pendulum clocks suspended on the same wall. By simple experiments he found that the synchronized state is a stable limit cycle of the system, because even after perturbing the system, the pendulums came back to this dynamic state. Originally Huygens thought, that this *odd kind of sympathy*, how he named it, occurs due to shared air currents between the pendulums. He performed several tests to confirm this idea. His experimental setup was really simple, with two pendulum clocks hanged on a common suspension beam which was placed between two chairs [7]. After performing some additional tests Huygens observed a stable and reproducible anti-phase synchronization, and attributed this to the imperceptible vibrations in the suspension beam. He summarized his observations in a letter to the Royal Society of London [8], and launched the study of synchronization phenomena and coupled oscillators.

Recent studies aimed to reconsider in various forms Huygens' two pendulum-clock experiment and realistically modeled the system. Bennet and his group [9] investigated the same two pendulum-clock system as Huygens did and came to the conclusion that as a function of the system's parameters several types of collective dynamics is observable. For strong coupling usually a "beat death" phenomena appears, where one pendulum oscillates and the other does not. For weak coupling, synchronization does not appear, and a quasi-periodic oscillation is observable. There is however an intermediate coupling strength interval where the anti-phase synchronization observed by Huygens appears. Huygens had thus some luck with his setup, because the coupling was just in the right interval: strong enough to cause synchronization, but also weak enough to avoid the "beat death" phenomenon.

Dilao [10] came to the conclusion that the periods of two synchronized nonlinear oscillators (pendulum clocks)

differ from the natural frequencies of the oscillators. Kurmon and his group [11] studied a similar system consisting of two pendulums, one of them having an exciting mechanism, and the two pendulums were coupled by a weak spring. Fradkov and Andrievsky [12] elaborated a model for such a system, and obtained from numerical solutions that both in- and anti-phase synchronizations are possible depending on the initial conditions.

Kapitaniak and his group [13] revisited Huygens' original experiment and found that the anti-phase synchronization usually emerges, although in rare cases in-phase synchronization is also possible. They also elaborated a more realistic model for this experiment [14].

Pantaleone [15] considered a similar system, but he used metronomes placed on a freely moving base instead of pendulum clocks. He simply modeled the metronomes as van der Pol oscillators [16] and came to the conclusion that anti-phase synchronization occurs in some rare cases only. He proposed this setup as an easy classroom demonstration for the Kuramoto model and extended the study for larger systems containing up to seven globally coupled metronomes. Recently Ulrichs and his group [17] examined the case when the number of metronomes was even larger.

The present work intends to continue this line of studies considering an ensemble of metronomes arranged symmetrically on the perimeter of a freely rotating disk, as illustrated in Figure 1. The free rotation of the disk acts as a coupling mechanism between the metronomes and for high enough ticking frequencies synchronization emerges. Our aim here is to investigate the conditions favoring such spontaneous synchronization in large ensembles of metronomes. In order to achieve our task, we first study the dynamics of the system by well-controlled experiments. Contrary with earlier studies that investigated the final stable dynamic state of the system, here we also consider and describe the transient dynamics leading to synchronization. We construct then a realistic model for the system and its modeling power is proved by comparing its results with the experimental ones. Finally, the model is used to investigate synchronization level and emergence of synchronization in large ensembles composed of identical metronomes.

II. EXPERIMENTAL SETUP

The experimental setup is sketched in Figure 1. The main units are the metronomes (Figure 1 and 3a), which are devices that produce regular, metrical beats. They were patented by Johann Maelzel in 1815 as a timekeeping tool for musicians ([18]). The oscillating element of the metronome is a physical pendulum, which consists of a rod with two weights on it (Figure 2): a fixed one at the lower end of the rod denoted by W_1 and a movable one W_2 , attached to the upper part of the rod. In general $W_1 > W_2$, and the rod is suspended on a horizontal axes between the two weights in a stable manner, so that the center of mass lies below the suspension axes.

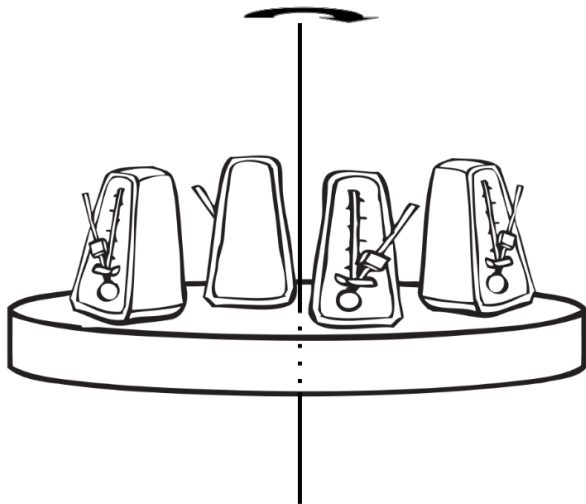


FIG. 1: *Schematic view of the experimental setup: metronomes are placed on the perimeter of a disc that can rotate around a vertical axes.*

By sliding the W_2 weight on the rod, the oscillation frequency can be tuned. There are several marked places on the rod where the W_2 weight has a stable position, yielding standard ticking frequencies for the metronome. These frequencies are marked on the metronome in the units: Beats Per Minute (BPM).

Another key part of the metronomes is the exciting mechanism, which has the aim to compensate the energy lost by frictions. This mechanism yields additional momentum to the physical pendulum in form of pulses delivered at a given phase of the oscillation period. For a more detailed analysis of this exciting mechanism we recommend the work of Kapitaniak et. al [14].

For the experiments we used the commercially available Thomann 330 metronomes (Figure 3a). From the 10 metronomes we had bought, 7 ones were carefully selected, so that their standard ticking frequencies be as similar as possible. Naturally, since there are no two identical units, in experiments we have to deal with a non-zero standard deviation of their natural frequencies.

In order to globally couple the metronomes, we placed

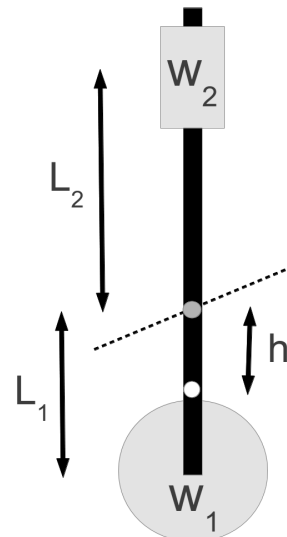


FIG. 2: *Schematic view of the metronomes' bob. The dotted line denotes the horizontal suspension axes, and the white dot illustrates the center of mass.*

them on a disk shaped platform which can rotate with a very small friction around a vertical axes, as it is sketched on Figure 1 and illustrated on the photo in Figure 3a.

In order to monitor separately the dynamics of all metronomes, photo-cell detectors (Figure 3b) were mounted on them. These detectors are commercial ones (Kingbright KTIR 0611 S), and contain a Light Emitting Diode and a photo-transistor. They were mounted on the bottom of the metronomes.

The wires starting from each metronome (seen in figure 3) connect the photo-cells with a circuit board, allowing data collection through the USB port of a computer. Data collection was done using a free, open-source program, called *MINICOM*. ([19]). The data is saved in log files, and can be processed in real-time. It is possible to follow simultaneously the states of up to 8 metronomes. The circuit board sends data just in those moments when there is a change in the signal from the photo-cell system (i.e. a metronome's bob passes the light-gate). In such moments it records a string like: 0 – 0 – 1 – 1 – 0 – 1 – 0 1450, where the first 7 numbers characterize the metronome bobs position relative to the photo-cell (whether the gate is open or closed) and the ninth number is the time, where one time unit corresponds to 64 microseconds. Since we are interested in the dynamics of this system from the viewpoint of synchronization, for numerical evaluation we will compute the classical order parameter, r , of the Kuramoto model [2]:

$$r \exp(i\phi) = \frac{1}{N} \sum_j \exp(i\theta_j). \quad (1)$$

Here ϕ is an average phase of the whole ensemble, θ_j is

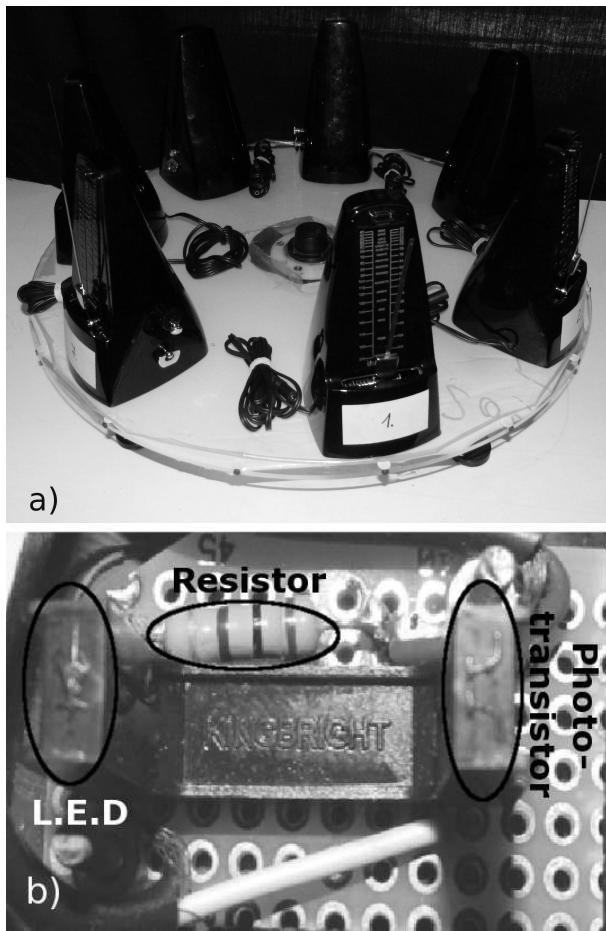


FIG. 3: (a) The experimental setup, with the metronomes placed on the platform and the wiring that carries information on the position of the metronomes' phases. (b) One of the used light-gates (Kingbright KTIR 0611 S), composed of an infrared LED and a photo-transistor.

the phase of the j -th metronome, N is the number of metronomes, and i is the imaginary unit.

From the recorded data we can get directly only those moments in which the metronomes' bobs pass through the light-gates, so some additional steps are needed in order to get the θ_j phases of all metronomes and to compute for given time moments the Kuramoto order-parameter. In order to achieve this, first we excluded from the data those time-moments when the metronome's bob passed the second time through the light-gate in one period, and after that we remained with the pass-times corresponding to a given directional motion only. With this "cleaned data" we calculated the period of each cycle and interpolated this time-interval for the θ_j phases (between 0 and 2π , corresponding to the state of a Kuramoto rotator), assuming a uniform angular-velocity. In such manner in each time-moment, the θ_j phase of each metronome (considered here as a rotator) can be uniquely determined and the Kuramoto order parameter (1) was computed.

$\omega(BPM)$	160	168	176	184	192	208
$\sigma(BPM \cdot 10^{-7})$	8.4	7.9	7.8	9.8	8.5	8.7

TABLE I: Standard deviation of the used seven metronomes for different frequencies

Before starting the experiments we monitored separately each metronome, and recorded their exact frequency for all the standardly marked rhythms. In such manner we have selected those 7 metronomes that had their standard frequencies relatively close to each other, and precisely measured these values. From these values the standard deviation of the metronomes' natural frequencies could be determined (Table I).

III. EXPERIMENTAL RESULTS

As already described in the introductory section, the metronomes oscillate with different natural frequencies, depending on the position of the adjustable weight on the metronomes' rod. For our experiments we have used the standard frequencies marked on the metronome. These frequencies are given in BPM units.

Before discussing in detail the experimental results, we have to emphasize, that independently of the chosen initial condition, only in-phase synchronization of the metronomes was observed. Reasons for this will be given in a separate section (Section VI).

In the very first experiments we were interested in studying how the chosen frequency influences the detected synchronization level. We fixed all the metronomes' frequencies on the same marked value and placed them symmetrically on the perimeter of the rotating platform as indicated in Figure 3a. Naturally, this does not mean that in reality their frequencies were exactly the same, since no two real macroscopic physical systems can be exactly identical. We initialized the system by starting the metronomes randomly, and let the system composed by the metronomes and platform freely evolve.

For each considered frequency value we made 10 measurements, collecting data for 10 minutes. The dynamics of the computed Kuramoto order parameter averaged on the 10 independent realizations are presented on Figure 4a.

The results suggest that by increasing the metronomes' natural frequencies, the degree of the obtained synchronization level increases. The standard deviations of the natural frequencies of the independent oscillators is indicated in Table I.

Since there is no clear trend in this data as a function of ω , the obtained result suggests that the observed effect is not due to a decreasing trend of the metronomes' standard deviation. We have also found that for the standard metronome frequencies below 160 BPM the system did not synchronize. It is interesting to note however, that if

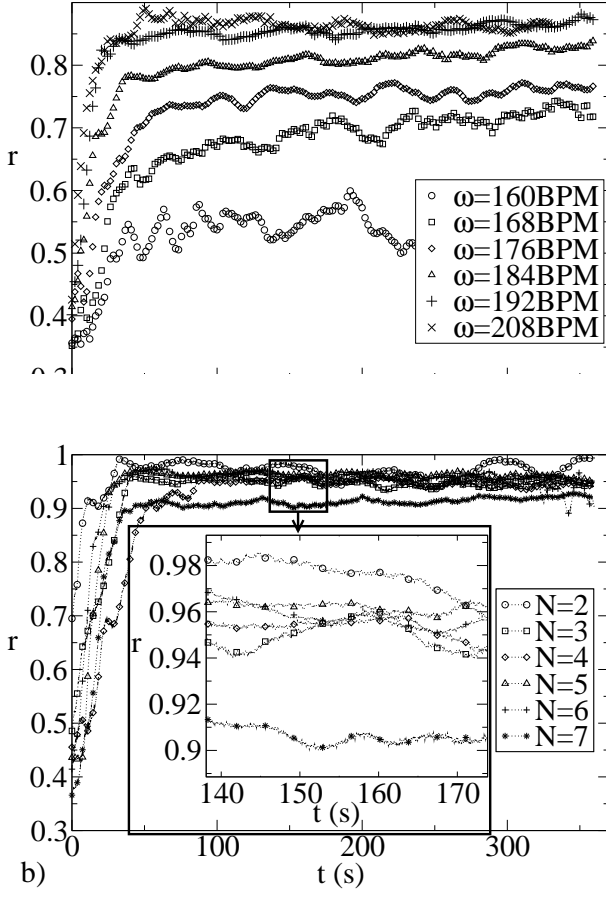


FIG. 4: Dynamics of the order parameter for different natural frequencies and metronome numbers. (a) Results for seven metronomes, different curves corresponding to different frequencies as indicated in the legends. (b) Results are for the same natural frequency (192 BPM) and different metronome number as indicated in the legend. On both graphs the results are averaged on 10 independent measurements.

one inspects only visually or auditory the system, he/she would observe no synchronization for frequencies already below 184 BPM. This means that we are not suited to detect partial synchronization with an order parameter below $r = 0.75$.

In a second experiment we were investigating the influence of the metronome number on the synchronization level. In order to study this, we have fixed the metronomes on the same frequency (192 BPM) and repeated the previous experiment with increasing number of metronomes placed on the rotating platform.

Again, for obtaining accurate results we performed 10 measurements for each configuration, and averaged the observed order parameter. The averaged results are presented on figure 4b.

Although the standard deviation of the metronomes' natural frequencies (Table II) does not present a clear trend as a function of the metronome number, N , we

N	2	3	4	5	6	7
$\sigma \text{ (BPM} \cdot 10^{-7})$	5.1	8.1	7.5	7.1	6.7	8.5

TABLE II: Standard deviation of the metronomes natural frequencies for different metronome number on the rotating platform.

get for the detected synchronization level a clear trend: increasing the number of metronomes will result in a decrease of the synchronization level.

IV. THEORETICAL MODEL

Inspired by the model described in [14], it is possible to consider a simple mechanical model for the system investigated here. The model is composed of a rotating platform and physical pendulums attached to its perimeter, as it is sketched on Figure 5.

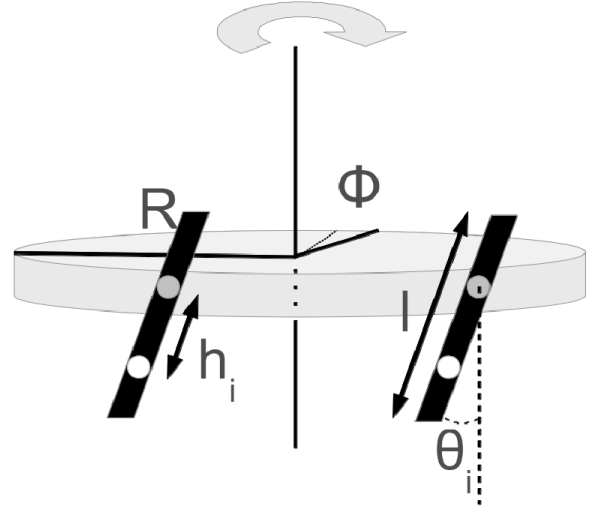


FIG. 5: Schematic view and notations for the considered mechanical model. The white dot denotes the center of mass of the physical pendulums and the gray dot is the suspension axis.

The Lagrange function of such a system writes as:

$$L = \frac{J}{2} \dot{\phi}^2 + \sum_{i=1}^N \frac{J_i \omega_i^2}{2} + \sum_{i=1}^N \frac{m_i}{2} \left\{ \left[\frac{d}{dt} (x_i + h_i \sin \theta_i) \right]^2 + \left[\frac{d}{dt} (h_i \cos \theta_i) \right]^2 \right\} - \sum_{i=1}^N m_i g h_i (1 - \cos \theta_i) \quad (2)$$

The first term is the kinetic energy of the platform, the second is the kinetic energy due to the rotation of the pendulum around its center of mass, the third one is the kinetic energy of the pendulum's center of mass, and the last term is the potential energy of the pendulum. In the Lagrangian we have used the following notations:

the index i denotes the pendulums, J is the moment of inertia of the platform with the metronomes on it – taken relative to the vertical rotation axes, ϕ is the angular displacement of the platform, m_i is the total mass of the pendulum ($m_i \approx W_1^{(i)} + W_2^{(i)}$, neglecting the mass of the rod), h_i is the distance between the center of mass and the suspension point of the pendulum, x_i is the horizontal displacement of the center of mass of the pendulums due to the rotation of the platform, θ_i is the displacement of the i -th pendulum's center of mass, in radians, J_i is the moment of inertia of the pendulum relative to its center of mass and ω_i is the angular velocity of the rotation of the pendulum relative to its center of mass. It is easy to realize that $x_i = R\dot{\phi}$ and $\omega_i = \dot{\theta}_i$. Assuming now that the mass of all the weights suspended on the metronomes bob are the same ($W_1^{(i)} = w_1$, $W_2^{(i)} = w_2$, and consequently $m_i = m$), and disregarding the $m_i g h_i$ constant terms, one obtains:

$$L' = \left(\frac{J + NmR^2}{2} \right) \dot{\phi}^2 + \sum_i \left(\frac{mh_i^2}{2} + \frac{J_i}{2} \right) \dot{\theta}_i^2 + mR\dot{\phi} \sum_i h_i \cos \theta_i \cdot \dot{\theta}_i + mg \sum_i h_i \cos \theta_i \quad (3)$$

The Euler-Lagrange equations of motion yields:

$$(J + NmR^2)\ddot{\phi} + mR \sum_i h_i [\ddot{\theta}_i \cos \theta_i - \dot{\theta}_i^2 \sin \theta_i] = 0 \quad (4)$$

$$[mh_i^2 + J_i]\ddot{\theta}_i + mR\ddot{\phi}h_i \cos \theta_i + mgh_i \sin \theta_i = 0. \quad (5)$$

The above equations of motion are for a Hamiltonian system where there is no damping (no friction) and no driving (excitation). Friction and excitation from the metronomes' driving mechanism has to be taken into account with some extra terms. The system of equations of motion writes as

$$(J + NmR^2)\ddot{\phi} + mR \sum_i h_i [\ddot{\theta}_i \cos \theta_i - \dot{\theta}_i^2 \sin \theta_i] + c_\phi \dot{\phi} + \sum_i \mathbb{M}_i = 0 \quad (6)$$

$$[mh_i^2 + J_i]\ddot{\theta}_i + mR\ddot{\phi}h_i \cos \theta_i + mgh_i \sin \theta_i + c_\theta \dot{\theta}_i = \mathbb{M}_i. \quad (7)$$

where c_ϕ and c_θ are coefficients characterizing the friction in the rotation of the platform and pendulums, and \mathbb{M}_i are some instantaneous excitation terms defined as

$$\mathbb{M}_i = M\delta(\theta_i)\dot{\theta}_i, \quad (8)$$

where δ denotes the Dirac function and M is a fixed parameter characterizing the driving mechanism of the metronomes. The choice of the form for \mathbb{M}_i in equation (8) means that excitations are given only when the metronome's bob passes the $\theta = 0$ position. The term $\dot{\theta}$ is needed in order to ensure a constant momentum input, independently of the metronomes amplitude. It insures

also that the excitation is given in the good direction (direction of the motion). It is easy to see that the total momentum transferred, \mathbb{M}_{trans} , to the metronomes in a half period ($T/2$) is always M :

$$\mathbb{M}_{trans} = \int_t^{t+T/2} M\delta(\theta_i)\dot{\theta}_i dt = \int_{-\theta_{max}}^{\theta_{max}} M\delta(\theta_i)d\theta_i = M$$

This driving will be implemented in the numerical solution as

$$\mathbb{M}_i = \begin{cases} M/dt & \text{if } \theta_i(t-dt) < 0 \text{ and } \theta_i(t) > 0 \\ -M/dt & \text{if } \theta_i(t-dt) > 0 \text{ and } \theta_i(t) < 0 \\ 0 & \text{in any other case} \end{cases}$$

where dt is the time-step in the numerical integration of the equations of motion. It is immediate to realize that this driving leads to the same total momentum transfer M , as the one defined by equation (8).

The coupled system of equations (6,7) can be written in a form more suitable for numerical integration:

$$\ddot{\phi} = \frac{mR \sum_i h_i \dot{\theta}_i^2 \sin \theta_i - c_\phi \dot{\phi} - \sum_i \mathbb{M}_i + A + B - C}{D}, \quad (9)$$

$$\ddot{\theta}_i = \frac{\mathbb{M}_i - mR\ddot{\phi}h_i \cos \theta_i - mgh_i \sin \theta_i - c_\theta \dot{\theta}_i}{mh_i^2 + J_i} \quad (10)$$

where

$$A = m^2 g R \sum_i \frac{h_i^2 \sin \theta_i \cos \theta_i}{mh_i^2 + J_i},$$

$$B = mRc_\theta \sum_i \frac{h_i \dot{\theta}_i \cos \theta_i}{mh_i^2 + J_i},$$

$$C = mR \sum_i \frac{h_i M_i \cos \theta_i}{mh_i^2 + J_i},$$

$$D = \left(J + NmR^2 - m^2 R^2 \sum_i \frac{h_i^2 \cos^2 \theta_i}{mh_i^2 + J_i} \right).$$

Now taking into account that the metronomes' bobs have the form sketched in Figure 2b and the L_1 distances are fixed and assumed to be identical for all the metronomes, the h_i and J_i terms of the physical pendulums in our model will be calculated as:

$$h_i = \frac{1}{w_1 + w_2} (w_1 L_1 - w_2 L_2^{(i)}) \quad (11)$$

$$J_i = w_1 L_1^2 + w_2 (L_2^{(i)})^2. \quad (12)$$

V. REALISTIC MODEL PARAMETERS

The parameters were chosen in agreement with the characteristic values of our experimental device: $w_1 =$

0.025 kg, $w_2 = 0.0069$ kg, $L_1 = 0.0358$ m, $L_2 \in [0.019, 0.049]$ m depending on the chosen natural frequency, $R = 0.27$ m and $J \in [0.0729, 0.25515]$ kg m² depending on the number of metronomes placed on the platform.

The damping and excitation coefficients were estimated as follows. For the estimation of c_θ , a single metronome on a rigid support was considered. Switching off the excitation mechanism, a quasi-harmonic damped oscillation of the metronome took place. The exponential decay of its amplitude as a function of time uniquely defines the damping coefficient, hence a simple fit of the amplitude as a function of time allowed the determination of c_θ . Switching now the exciting mechanism on, leads the metronome to a steady-state oscillation regime with constant amplitude. Since c_θ has already been measured, this amplitude value is defined by the excitation coefficient M . Solving equations (6) and (7) for a single metronome and tuning it until the same steady-state amplitude is obtained as in experiments makes possible the estimation of M . Now that both c_θ and M are known, the following scenario is considered: all the metronomes are placed on the platform and synchronization is reached. Then the platform has a constant-amplitude oscillatory motion. In order to determine c_ϕ , its value is tuned while solving the equations (6)-(7) until the same amplitude of the disc's oscillations is obtained as in experiments. This way all the parameters in the model can be related to the experimental quantities. Using the above defined method, we estimated the following parameter values: $c_\theta = 0.00005$ kg m²/s, $c_\phi = 0.00001$ kg m²/s and $M = 0.000095$ Nm/s.

VI. IN-PHASE SYNCHRONIZATION VERSUS ANTI-PHASE SYNCHRONIZATION OF TWO METRONOMES

As it is described in the introductory section, in the case of two coupled oscillators many previous works have reported a stable anti-synchronized state [9, 12, 13]. Due to the fact that independently of the starting condition no such stable phase was observed in our experiments, we feel that investigating this issue is important. Starting from our theoretical model described in section IV, we will show that the in-phase synchronization is favored, whenever there are equilibrated damping and driving forces acting on the metronomes.

Let us investigate first the case without any damping and with no driving forces. The equations of motion for such a system are given by equations (4) and (5). Considering the case of two metronomes ($N = 2$) with small-angle deviations ($\theta_{1,2}^{max} \ll \pi/2$), we investigate the synchronization properties of such a system. The synchronization level will be studied here by an appropriately chosen order parameter for two metronomes, z , that indicates whether we have in-phase or anti-phase synchronization. The Kuramoto order parameter is not

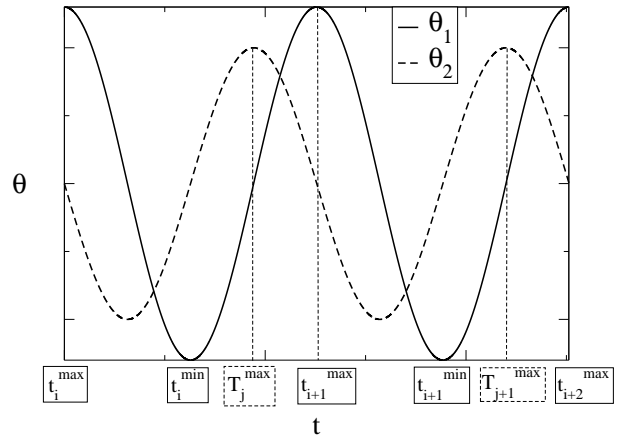


FIG. 6: Dynamics of two metronomes as a function of time, and the quantities used for defining the z order parameter

appropriate for such purpose, since it cannot distinguish between the totally unsynchronized and the anti-phase synchronized dynamics. In order to introduce a proper order parameter, let us consider the dynamics of two metronomes as a function of time by plotting $\theta_{1,2}(t)$ (Figure 6). Let us denote by t_i^{min} and t_i^{max} the time-moments where metronome 1 has local minimum and maximum θ_1 values, respectively. We denote by T_j^{max} the time-moments where metronome 2 has local maximum θ_2 values. With these notations, we define the following two time-like quantities, that are characterizing the average time-interval of the maximum position of the $\theta_2(t)$ relative to the maximum and minimum positions of $\theta_1(t)$, respectively:

$$t_1 = \langle \min_{\{i\}} \{ |t_i^{max} - T_j^{max}| \} \rangle_j \quad (13)$$

$$t_2 = \langle \min_{\{i\}} \{ |t_i^{min} - T_j^{max}| \} \rangle_j \quad (14)$$

In the equations from above the averages are considered for all j maximum positions of $\theta_2(t)$, and the "min" notation refers to the minimal value of the quantity in the brackets. Now, the z order parameter is defined as:

$$z = \frac{t_2 - t_1}{t_2 + t_1} \quad (15)$$

It is easy to realize that z is bounded between -1 and 1 . For a totally in-phase synchronized dynamics we have $t_1 = 0$, leading to $z = 1$. For a totally anti-phase synchronized dynamics $t_2 = 0$, and we get $z = -1$. Negative z values suggest a dynamics where the anti-phase synchronized states are dominant, positive z values suggest a dynamics with more pronounced in-phase synchronized states.

The z order parameter was estimated numerically for different initial conditions. A velocity Verlet-type algorithm was used, and simulations were performed up to a

$t = 10000$ s time interval, with a $dt = 0.1$ s time-step. (We remark, that this time-step is sufficiently small, since for $dt = 0.001$ s we obtained very similar results.)

Initially the deviation angle of the first metronome was chosen as $\theta_1(0) = \theta_{max} = 0.1$ rad and $\theta_2(0)$ was chosen in the interval $[-0.1, 0.1]$ rad, leading to various initial phase-differences between them. The obtained z values as

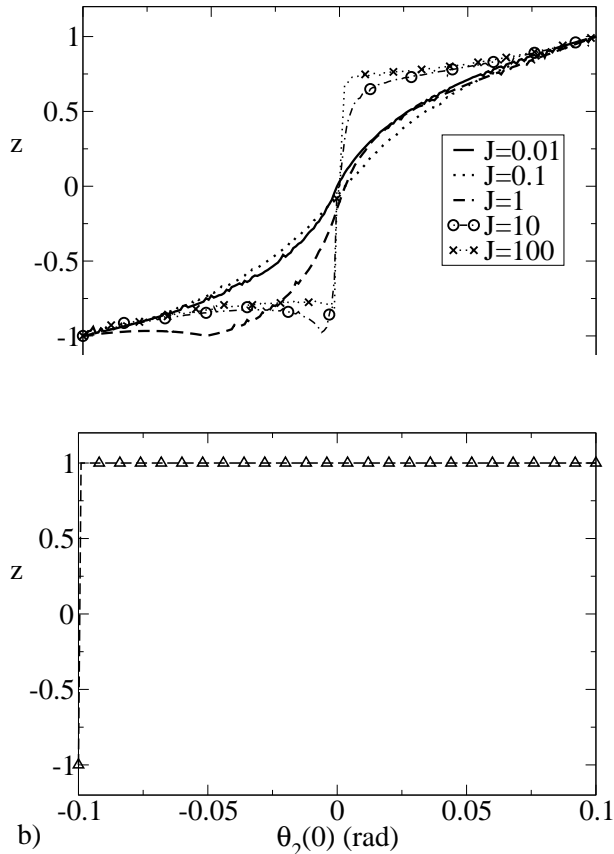


FIG. 7: The z order parameter as function of the initial phase $\theta_2(0)$ of metronome 2. (a) Simulation results without damping ($c_\theta = 0$, $c_\phi = 0$) and no driving ($M = 0$). (b) Simulation results with the realistic damping and driving parameters given in Section V.

The obtained results suggest that for the friction-free case with no driving (Figure 7a), depending on how the dynamics is initialized, both the synchronized and anti-synchronized states are observable. If the anti-phase initial condition is closer, the dynamics will be mostly anti-phase synchronized. Consequently, if the initial condition is closer to the in-phase synchronization, the dynamics will be mostly in-phase synchronized. Increasing the inertial momenta of the platform will lead to a better synchronization level. In case both damping and driving is present and the parameters are the ones experimentally measured in the system (Figure 7b), the anti-phase synchronization is suppressed and only in-phase synchronization appears. Anti-phase synchronization is unlikely

to be observed, this will appear only in the case when the two metronomes are started exactly in anti-phases ($\theta_2(0) = -\theta_1(0)$).

In view of these results, one can understand why in our experiments only the in-phase synchronized dynamics was observed.

VII. SIMULATION RESULTS FOR SEVERAL METRONOMES

The equations of motion (9,10) were numerically integrated using a velocity Verlet-type algorithm as integration method. A time-step of $dt = 0.1$ s was chosen. As a test of the model, first we tried to reproduce the experimental results. Our first simulation is intended to reproduce the experimental results presented in Figure 4. Seven metronomes with the same natural frequencies as the experimentally measured ones were considered, and the time-evolution of the Kuramoto order parameter was computed. Results for different frequency values are presented in Figure 8a.

Except for the first maximum, the trends are in good agreement with the experimental results from Figure 4. We believe that this maximum appears due to the differences in the initialization of the dynamics in the experiments and simulations.

As a second simulation experiment, we have studied the time-evolution of the order parameter for different pendulum number, setting the same 192 BPM natural frequency as in the experiments. Again, similarly to the experiments, we averaged the results for 10 independent simulations. The obtained trend is sketched on Figure 8b.

The trend of the simulation results is in agreement with the experimental ones: increasing the metronomes' number results in a decrease in the observed synchronization level. In simulations however, this decrease is not as evident as in the experiments. We believe that the difference is due to the simplified manner how the slight differences between the metronomes are handled in the simulations. We recall that in the model, the differences between metronomes is included only via the $L_2^{(i)}$ terms. In reality the other parameters of the metronomes can also differ.

These simulation results suggest that we have a reasonable model for understanding the synchronization in such a system. One can investigate thus by simulations several interesting cases, that are not feasible in the experiments. Many interesting questions can be formulated in such manner. In the following we will focus however only on clarifying the problems that we have experimentally investigated, namely the influence of the number of oscillators and the chosen natural frequency on the observed synchronization level. Computer simulations will allow us to consider a high number of oscillators and will also allow a continuous variation of the metronomes' natural frequencies. Particularly, we are interested in clari-

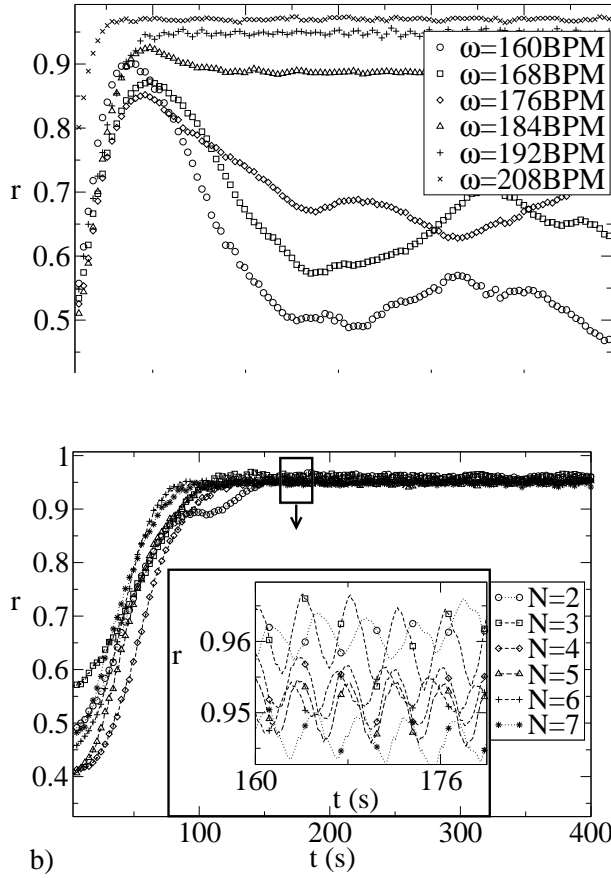


FIG. 8: Simulation results for the time-evolution of the Kuramoto order-parameter. (a) The curves represent results for the same natural frequencies, as the ones used in experiments. (b) Results for the same pendulum number as the ones used in experiments. For both graphs the presented results are an average over 10 independent simulations.

fying how the stable synchronization level is varying as a function of the metronomes' number, and how the characteristic time needed to achieve synchronization varies as a function of the metronomes' number.

First we have reconsidered the results presented in Figure 8b and investigated the system for large number of metronomes. Also, for the sake of a better accuracy we considered an average over 100 simulations for each fixed N values. The same 192 BPM natural frequency was fixed for all oscillators. Simulations with up to $N = 256$ metronomes were considered and the obtained results are presented on Figure 9a.

The results confirm our previous conclusion: increasing the metronomes number will result in a decrease in the observed synchronization level. However, a quantitative analysis of the results suggests that in the limit of $N \rightarrow \infty$ (we considered up to 1024 metronomes) the Kuramoto order parameter converges to a non-zero value. Comparing the results from Figure 9a with the ones presented in Figure 8b confirms also what one would natu-

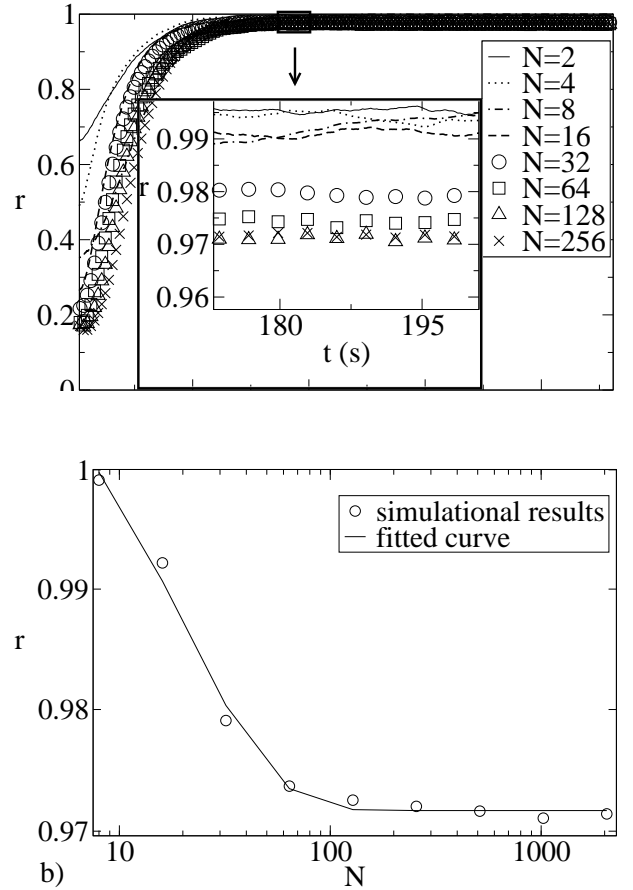


FIG. 9: Simulation results for the equilibrium synchronization level. (a) Time-evolution of the r order parameter for different pendulum number, as indicated in the legend. One graph is obtained after an average on 100 independent simulations. (b) The r order parameter as a function of the pendulum number. The circles indicate the simulation results and the continuous curve shows the fit (16) with parameters: $a = 0.041$, $b = 0.049$ and $c = 0.971$.

rally expect based on the Kuramoto model: considering totally identical metronomes with no standard deviation of their natural frequencies, leads to an increased Kuramoto order parameter. Simulations suggest that the values of the stabilized order parameter converge exponentially to a stable $c = 0.971$ value

$$r(N) = a \exp(-bN) + c, \quad (16)$$

with the best fit parameters $a = 0.041$, $b = 0.049$. On Figure 9b we plot this N dependence, and indicate also the fit given with the above mentioned parameters.

The results from above prove that by increasing the number of metronomes placed on the rotating platform the partial synchronization survives. The system converges to a dynamic state with a non-zero synchronization order parameter. We have also learned from Fig-

ure 9 that the equilibrium value of the order parameter does not vary too much by increasing the number of metronomes. In contrast with this small variation, the time needed to achieve synchronization increases more evidently. In order to define a characteristic time needed to achieve synchronization, we define an averaged order parameter, q , that is suitable to capture the initial part of the time-evolution:

$$q = \int_{dt}^{t_{max}} \frac{r(t)}{t} dt, \quad (17)$$

Here dt is the integration time-step for the equations of motion and t_{max} is roughly the time-length of the considered simulation.

This order parameter is a weighted average on the $[dt, t_{max}]$ interval, where the weight factors are favoring the initial time-moments. As a result of this, this order parameter captures the initial transient part of the dynamics. When the value of the Kuramoto order parameter does not change significantly (the case when the number of metronomes, N , were varied) the q order parameter is appropriate for revealing the dynamics in which synchronization is achieved quicker. Consequently, a characteristic time, t_c , to achieve synchronization can be defined as: $t_c = 1/q$. Naturally, the value of q and t_c depend on both the dt and t_{max} values (the limits in the integral (17)). The good news however is, that although the values are dependent on the chosen dt and t_{max} values, seemingly there is a scaling of q as a function of N :

$$q = \frac{1}{t_c} = C \cdot N^{-1/2} + K(t_{max}) \quad (18)$$

Results confirming this scaling are presented in Figure 10. Simulations yield the $C = 5.55$ constant. Experimental results plotted on Figure 10b indicate the same scaling. Moreover, the slope of the linear fit gives $C = 5.38$ in excellent agreement with the simulation results.

Computer simulations allow us also to investigate in more detail the dependence of the r and q order parameter as a function of the natural frequencies of the pendulums. Results for different pendulum number are given in Figure 11. These results confirm again, that by decreasing the metronomes' natural frequency the synchronization level decreases. Increasing the metronome number and/or by decreasing their natural frequencies makes harder and harder to achieve a synchronized state.

VIII. CONCLUSIONS

The dynamics of a system composed of coupled metronomes was investigated both by simple experiments and computer simulations. We were interested in finding

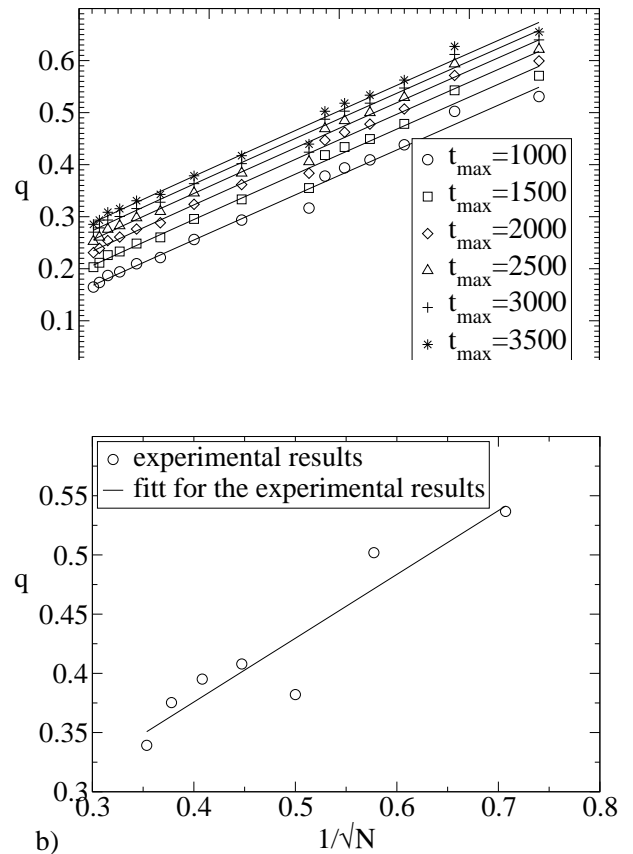


FIG. 10: *Scaling of the q order-parameter. (a) Symbols are simulation results for various t_{max} values, and the curves are linear fits. One can observe that the slopes are roughly the same, and the linear fit is a good approximation. (b) Scaling for the experimental results.*

the conditions for an emerging synchronization. Contrarily with many previous studies, here the problem was analyzed not from the viewpoint of dynamical systems, but from the viewpoint of collective behavior and emerging synchronization.

The experiments suggested that there is a limiting natural frequency of the metronomes below which spontaneous synchronization is not possible. By increasing the frequency above this limit partial synchronization will emerge. The obtained synchronization level increases monotonically with increasing the natural frequency of the oscillators. The experiments proved that by increasing the number of metronomes in the system the final stable synchronization level drops and the time needed to achieve the final dynamical equilibrium state increases.

In order to better understand the dynamics of the system a realistic model was build. The parameters of the model were fixed in agreement with the experimental conditions and the equations of motion were numerically integrated. The model proved to describe well the experiments, and reproduced the experimentally observed trends. The model allowed a fine verification of our find-

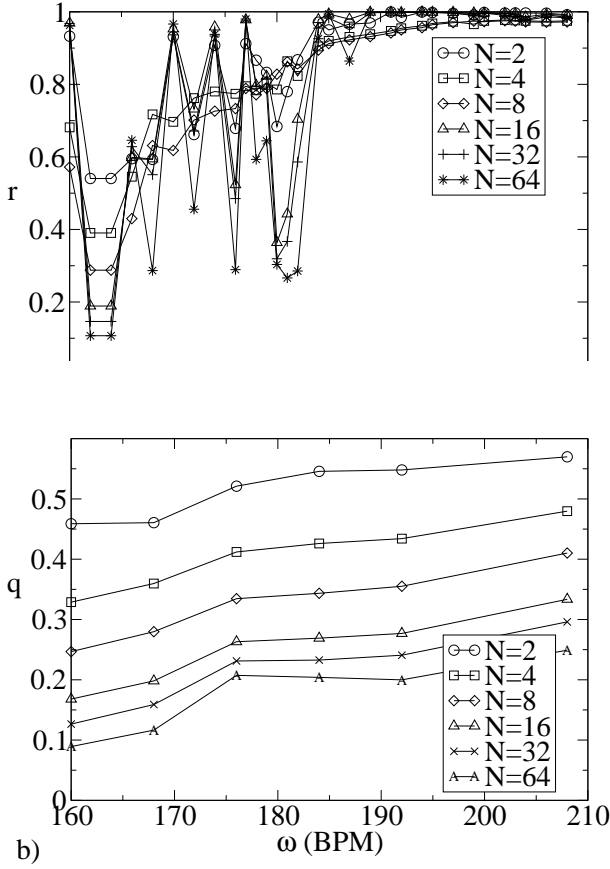


FIG. 11: Simulation results for the influence of the metronomes natural frequencies ω on the obtained synchronization level, measured by the r (Figure a) and q (Figure b) order parameters. Different curves are for different metronome number, as indicated in the legends.

ings regarding the conditions under which spontaneous synchronization emerges. It was found that by increasing the number of metronomes in the system the synchronization level converges exponentially to a stable limit. Also, it was found that the time needed to achieve synchronization scales in a universal manner with the number of metronomes placed on the rotating platform.

The successes of the elaborated model opens an easy way for many further studies regarding the dynamics of this system. Indeed, many other interesting questions can be formulated regarding the influence of the metronomes and rotating platform parameters on the obtained synchronization level and the observed trends. Also, one can study systems where the metronomes or groups of metronomes are fixed to different natural frequencies, or where there is an external driving on the system. The elaborated model has the advantage that the equations of motion are easily integrable and the model parameters are realistic having a direct connection to the parameters of an experimentally realizable system.

Finally, we hope that the novel experimental setup and the results presented here will help in clarifying some aspects for one of the oldest problem in physics, namely the spontaneous synchronization of coupled pendulum clocks. Although several similar problems have been considered in previous studies, we have shown that there are still many fascinating aspects that one can investigate in such simple mechanical systems.

IX. ACKNOWLEDGMENTS

Work supported by the Romanian IDEAS research grant PN-II-ID-PCE-2011-3-0348. The work of B.Sz. is supported by the POSDRU/107/1.5/S/76841 PhD fellowship.

-
- [1] S. Strogatz, *Sync: The Emerging Science of Spontaneous Order* (Hyperion, New York, 2003)
 - [2] Y. Kuramoto and I. Nishikawa, *J. Stat. Phys.* **49**, 569 (1987)
 - [3] R. Mirollo and S. Strogatz, *SIAM J. Appl. Math.* **50**, 1645 (1990)
 - [4] S. Bottani, *Phys. Rev. E* **54**, 2334 (1996)
 - [5] S. Strogatz, *Physica D* **226**, 181 (2000)
 - [6] Z. Neda, A. Nikitin, and T. Vicsek, *Physica A* **321**, 238 (2003)
 - [7] A. Pikovsky, M. Rosenblum, and J. Kurths, *Synchronization: A Universal Concept in Nonlinear Science* (Cambridge University Press, Cambridge, England, 2002)
 - [8] C. Huygens, *Societe Hollandaise Des Sciences* (1665)
 - [9] M. Bennet, M. F. Schatz, H. Rockwood, and K. Wiesenfeld, *Proc. Roy. Soc. London A* **458**, 563 (2002)
 - [10] R. Dilao, *Chaos* **19** (2009)
 - [11] M. Kumon, R. Washizaki, J. Sato, R. K. I. Mizumoto, and Z. Iwai, *Proceedings of the 15th IFAC World Congress, Barcelona* (2002)
 - [12] A. L. Fradkov and B. Andrievsky, *Int. J. Non-linear Mech.* **42**, 895901 (2007)
 - [13] K. Czołczynski, P. Perlikowski, A. Stefanski, and T. Kapitaniak, *International Journal Bifurcation and Chaos* **21** (2011)
 - [14] K. Czołczynski, P. Perlikowski, A. Stefanski, and T. Kapitaniak, *Physica A* **388**, 5013 (2009)
 - [15] J. Pantaleone, *Am. J. Phys.* **70**, 9921000 (2002)
 - [16] B. van der Pol, *Philos. Mag* **3**, 64 (1927)
 - [17] H. Ulrichs, A. Mann, and U. Parlitz, *Chaos* **19**, 043120 (2009)
 - [18] Wikipedia, *Metronom* (2012 (accessed July 23, 2012)), <https://en.wikipedia.org/wiki/Metronome>
 - [19] Wikipedia, *Minicom* (2012 (accessed January 14, 2012)), <https://en.wikipedia.org/wiki/Minicom>